Journal of Manufacturing Systems 68 (2023) 644–650

Contents lists available at ScienceDirect

Journal of Manufacturing Systems

journal homepage: www.elsevier.com/locate/jmansys

Energy-efficient and quality-aware part placement in robotic additive manufacturing☆

Suyog Ghungrad [a], Abdullah Mohammed [b], Azadeh Haghighi [a,*]

[a] Mechanical and Industrial Engineering, University of Illinois Chicago, Chicago 60607, United States
[b] Department for Applied Computing and Engineering, Cardiff Metropolitan University, Cardiff, United Kingdom

ARTICLE INFO

Keywords:
Robotic additive manufacturing
Part placement
Energy consumption
Deviation error

ABSTRACT

The advancements in autonomous robots for additive manufacturing (AM) are opening new horizons in the manufacturing industry, especially in aerospace and construction applications. The use of multiple robots and collaborative work in AM has rapidly gained attention in the industry and research community. Addressing the process planning challenges for single-robotic AM is foundational in addressing more advanced challenges at the collaborative multi-robotic level for AM. Among these challenges include the part placement problem which explores the optimal positioning of the part within the robot's reach volume. The majority of the existing part placement algorithms take into account the part accuracy and manufacturing time for decision-making, while neglecting the implications of such decisions on energy efficiency and environmental sustainability. To address this gap, this paper presents a methodology for energy-efficient, high-quality part placement (EEHQPP) in robotic additive manufacturing. An energy-quality map is formulated and established to characterize the energy and quality variations across the robot's workspace to inform the decision-making process. Two case studies (a container and a spur gear) are considered, and the performance of the proposed approach compared to the benchmark (i.e., default part placement by the 3D printing software) are evaluated. The proposed algorithm reduces both the energy consumption and maximum deviation error of the container (6.5% and 19.4%, respectively) and spur gear (1.4% and 32.7%, respectively) geometries manufactured by the robotic additive manufacturing system.

1. Introduction

Robotic additive manufacturing (AM) is becoming popular due to the advancements of autonomous industrial robots, opening up new avenues, especially in the construction industry [1,2]. These robots are extremely beneficial as they are reliable and versatile, with the capability to perform multiple tasks or processes simultaneously by adjusting the end effectors [3]. Additional enhancements in AM through robotic manipulators are multi-directional fabrication [4], conformal deposition [5], and supportless printing [6]. Among the various robotic solutions, articulated robots offer an advantage over gantry-based robots in that they are comparatively smaller in size and are more flexible due to their higher degrees of freedom (DOF), making them a unique candidate for collaborative robotic 3D printing for on-site manufacturing, repair, and construction.

Part placement and trajectory planning which includes the decision on the optimal location and orientation of the part and robot trajectories, are generally among the main questions to be addressed by any robotic manufacturing process. This problem, however, will get reversed in collaborative additive manufacturing, as generally the part will be considered fixed, and the location of robots with respect to the part are decided. Both problems share similarities and thus, solving the part placement in single robot AM scenario would facilitate the robot placement in multi robot AM scenarios.

The idea of part placement for minimizing part build time [7], reducing trajectory execution error [8] or obtaining optimal orientation [9] for better quality has been studied for traditional manufacturing [10,11] as well as AM for enhancing accuracy [12]. Establishing different types of maps such as the stiffness [13] and deformation [14] maps, have proven to be helpful for addressing these questions. These maps address

* Corresponding author.
E-mail address: ahaghi3@uic.edu (A. Haghighi).

https://doi.org/10.1016/j.jmsy.2023.05.019

Available online 31 May 2023

the low stiffness of robots, the most significant factor in machining accuracy and stability, which is mainly caused by external forces during processes such as milling [15]. However, these maps would be less applicable in AM, as external forces acting on the manipulator would not necessarily be applicable in additive manufacturing. For novel robotics applications, more versatile types of maps have been designed based on robot dynamics, such as manipulability, capability, and kinematic reachability. These maps are particularly used in addressing the inverse problem of part placement, i.e., robot positioning, which involves accounting for the complex movements of high-degree-of-freedom robots and avoiding singularities along their paths [16]. The aim of these maps is to ensure that robots can reach their intended locations with greater ease and maneuverability. While these maps were originally developed for simple path applications, researchers have adapted them for traditional manufacturing applications such as cutting [17]. However, using these maps specifically for additive manufacturing processes can be challenging, as it requires different types of constraints and objective functions [18].

Moreover, as the energy consumption by industrial robots is on the rise [19], in addition to accuracy [20] and time [21], energy consumption by industrial robots should be an important factor in deciding part placement towards sustainable manufacturing. There have been some research studies on energy efficiency in industrial robots for traditional manufacturing. For example, with many simplifications in machining operations, an energy model for energy consumption of machine tool in machining process via 5 DOF machine was proposed in 2012 [22]. A particle swarm optimization algorithm for path optimization in spot welding based on shortest path and energy consumption was proposed [23]. A review paper discusses energy saving methods from hardware and software perspectives in robotic systems [24] and in the literature, most energy-minimizing algorithms of industrial robots exist for applications other than AM such as pick-and-place [25,26] or for entire robotic cell in manufacturing [27]. There exists a gap in establishing part-placement algorithms with both consideration of quality and energy in robotic AM applications, and eventually establishing a sustainable collaborative framework for mobile collaborative 3D printing robots as also highlighted in [28]. This paper is an attempt to fill this gap by proposing a quality-aware and energy-efficient part placement algorithm for robotic AM. It will become a foundation for more innovative and intelligent systems for multi-robot AM.

This work proposes a systematic approach for finding energy-efficient part placement within the robot's workspace for high-quality AM based on the robot's kinematics and print deviation error. For calculating this energy and deviation error, robot's energy consumption and robot's positional accuracy is, respectively, utilized. An energy-quality (EQ) map is established and presented to show the energy and quality variations across the robot's workspace. The rest of this paper is organized as follows: Section 2 describes the methodology for energy and quality characterization in robotic AM, as well as the proposed energy-efficient high-quality part placement algorithm. The case study parameters including the studied geometries, robot specifications and kinematics, and print parameters are presented in Section 3. Finally, the proposed algorithm is compared with the default placement (benchmark) by the standard 3D printing software in Section 4. Finally, the conclusion and future works are discussed in Section 5.

2. Methodology

In this section, the manipulator's energy consumption and the print quality (i.e., deviation error) are first characterized as a function of the robot's joint configuration. Next, an algorithm and an accompanying optimization problem for minimizing the robot energy consumption under the provided part tolerance requirements/constraints and robot kinematics is formulated and solved to determine the optimal part placement within the robot's reach. Fig. 1 illustrates the overall steps of the proposed approach.

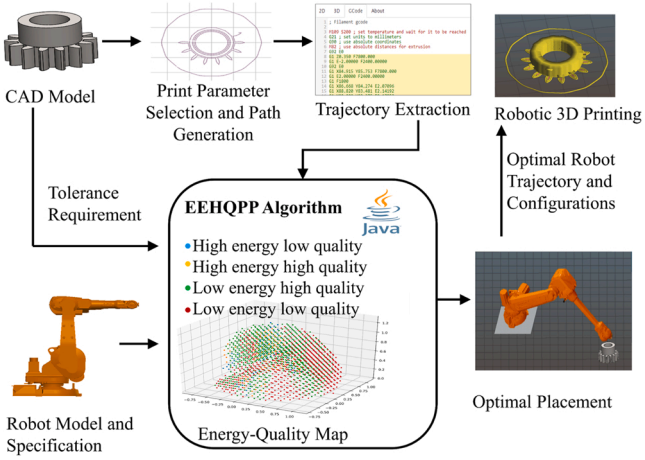

Fig. 1. Overview of the proposed methodology for part placement in robotic AM.

2.1. Energy module

The energy consumed by the robotic AM can be split into AM energy and manipulator energy. The AM energy is the energy required to print the part, which includes the printing energy, pre-heating of material or platform, and other miscellaneous energy [29]. The manipulator energy is the energy consumed by the manipulator to move along the trajectory. The AM energy needed to print the part is assumed to be similar for different part placements. This is since the energy required for most tasks like heating and maintaining the temperature of the platform would be the same irrespective of part location on the platform, without making any change to the print and printer settings [30]. However, the manipulator's energy consumption depends on the joint configuration and trajectory [31] as defined by the AM process. Building energy consumption models by utilizing several losses, such as mechanical friction and electrical (core, stator, windage and friction and etc.) exists [32–34]. However, efficient use of energy by utilizing robot kinematics and dynamics is possible and it is more beneficial than utilizing losses in controlling applications [35]. Hence, in this study, energy consumption model based on robot kinematics and dynamics is explored. The energy consumption $\mathbb{E}$ is calculated for path of length $d_{\lambda N}$ during λ^{th} time interval for the path which is divided into N intervals.

$$\mathbb{E} = \int_{\lambda_0}^{\lambda_N} \mathbb{P}(t)dt = \sum_{\lambda=0}^{N} \mathbb{P}(\lambda).dt \tag{1}$$

where power consumption ($\mathbb{P}$) is calculated by summing the power consumed by each joint ($\wp_i$) in the specific time interval (λ) as shown in Eq. 2.

$$\wp_i(\lambda) = \tau_i(\lambda).\dot{\theta}_i(\lambda)$$

$$\mathbb{P}(\lambda) = \sum \wp_i(\lambda) \tag{2}$$

where τ_i is the torque and $\dot{\theta}_i$ is the angular velocity of the i^{th} link. The torques τ_i has direct relationship with the angular acceleration and angular velocity of the links. Both the angular acceleration and angular velocity of the links can be calculated from the rotation of the links. The transformation matrix consists of the rotation and position information of the link i with respect to link h and it is a function of joint values (θ). The transformation matrix for a 6 DOF industrial robot can be expressed as [36],

$${}^{i}_{h}T(\theta) = \begin{bmatrix} {}^{i}_{h}R & P_i \\ 0 & 1 \end{bmatrix} \tag{3}$$

where ${}^{i}_{h}T$ is the transformation matrix between link i and link h, the ${}^{i}_{h}R$ and P_i are respectively rotation matrix and position vector. A forward backward recursive algorithm is necessary where forward recursion from first link to last link calculates linear and angular motion and inverse recursion from last link to first link calculates forces and torques of each link of the robot. Hence, it can be said that the energy consumption $\mathbb{E}$ is a function of joint angles (θ) and which can be represented as,

$$\mathbb{E} = \mathscr{F}(\theta) \tag{4}$$

The forward kinematics (FK) is used to find the end-effector coordinates of the robot from a given joint configuration and inverse kinematics (IK) computes the joint configurations to reach a desired position in the workspace. Inverse kinematics is performed at each point in the workspace to obtain joint positions, velocities, and accelerations. Solving inverse kinematics for the six DOF manipulators creates 0–8 possible solutions for the joint configurations with zero meaning that the robot cannot reach the desired point. Additionally, selecting among the different possible joint configurations, simply the configuration with the lowest energy consumption is chosen [35].

2.2. Quality module

Positional accuracy and repeatability are the most critical attributes of autonomous robots for manufacturing tasks [37]. Accurate positioning of the end-effector is highly desired in AM, as the manufactured parts need to have good dimensional accuracy [38]. As described previously, the end-effector's position with respect to the robot's base can be calculated from the forward kinematics of the robot's joint configurations.

$$X = FK(\theta) \tag{5}$$

where $\theta = [\theta_1, \theta_2, \ldots \theta_i]^T$ is the vector containing the i joint angles for i DOF manipulator and X is the vector containing the workspace position and orientation. The accuracy can be defined as the deviation between the desired position of the end-effector and the position it attains. This deviational error (e_w) at a waypoint w as shown in the Fig. 2 can be mathematically expressed as:

$$e_w = X_{actual} - X_{desired}$$

$$e_w = FK(\theta_w + d\theta_w) - FK(\theta_w) \tag{6}$$

where the $d\theta_w$ is the change or error in joint angles. The joint resolution errors caused by sensors plus motors and angular errors caused by calibration of D-H parameters of the manipulators will be systematic error and a same error value will be repeated. The controller errors for erroneous velocity and acceleration of the joints can lead to a change in the end-effector's position. However, in material extrusion AM, usually the deposition of material is at a constant rate and the end-effector's speed is low so the acceleration errors can be ignored. So, the error in joint angles at w^{th} waypoint can be expressed as [12]:

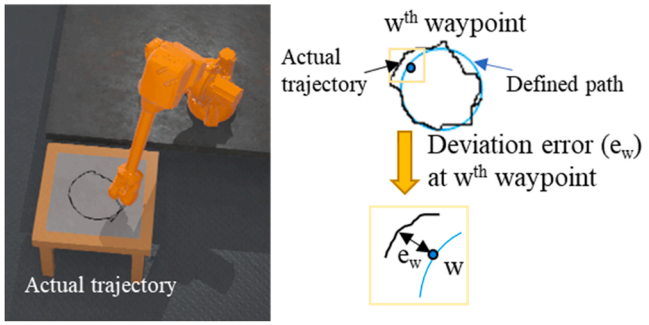

Fig. 2. Position error of end-effector for robotic additive manufacturing.

$$d\theta_w = \theta^c_w + k \bullet \dot{\theta}_w \tag{7}$$

where θ^c_w and k are the constant error gain values for systematic errors and erroneous velocity which can be obtained from experiments. Assuming for a small error in joint angles for short time interval for moving from w to $w+dw$, the deviation error in end-effectors position e_w can be defined as:

$$e_w = J \bullet d\theta_w$$

$$e_w = J \bullet \theta^c_w + J \bullet k \bullet \dot{\theta}_w \tag{8}$$

where J is the jacobian of the manipulator. Finding the deviation error for the trajectory will be key in achieving good quality parts. The allowable deviations while fabricating the part depends on the tolerance limit of the part. So, in this work, the quality of part is determined by the maximum deviation along the path defined from the CAD model.

$$\mathscr{E} = Max(e_w) \tag{9}$$

2.3. Energy-efficient high-quality part placement (EEHQPP) algorithm

The aim is to leverage the energy and quality modules and their outputs to determine the optimal print location (for a given print orientation) which consumes the least energy during the print while at the same time satisfies the print tolerance and quality requirements. We formulate this problem as a single-objective optimization problem with respect to the energy function while incorporating the quality requirements within the problem constraints. We adopt a single-objective and not a multi-objective optimization since quality is always defined with respect to the product tolerance. Therefore, as long as the formulated maximum deviation error is within the tolerance threshold, we are not interested in further reducing the error as such further error reductions might as a trade-off increase the overall energy consumption by further shifting the location of the print into the high-energy consumption zones of the robot. We consider the term good/high quality to refer to solutions with acceptable quality considering the provided tolerance limits and the term bad/low quality to refer to solutions with unacceptable quality considering the provided tolerance limits.

The following constraints are considered for the formulation of the optimization problem:

- Quality constraint: The print quality is affected by the robot's kinematics, as formulated in Section 2.2. A quality constraint ensures that dimensional and geometrical requirements of the part are satisfied and so the maximum error $\mathscr{E}$ should be within the tolerance limit of the part.
- Collision constraint: The collision constraint is to ensure that no collision occurs between manipulator, AM head, printed part, or ground surface at the part placement location. For this constraint, a clearance is given to them in all three directions.
- Print consistency constraint: To maintain controlled extrusion in AM, the manipulator is constrained with any sudden change in the velocity of the extrusion head while printing. Also, the velocity of the extrusion head should be within the selected AM extrusion limits and determined to ensure that adequate inter-layer and intra-layer bonding occurs during the printing process. As slight oscillations in the desired velocity are unavoidable [39], a constraint on the upper limit is applied to ensure even and smooth printing.
- Robot design constraint: The design constraints of the robot's links, such as angles or rotation, velocity, and acceleration based on the adopted robot model and its specifications.

Finally, the objective function is the total energy consumed to print the geometry by the manipulator, which is a function of joint configurations as shown in Section 2.1. The problem formulation is as follows:

$$Minimize : \mathbb{E} = \mathscr{F}(\theta) \tag{10}$$

subject to:

Quality constraint:

$$\mathscr{E} < \mathscr{T} \tag{11}$$

Print consistency constraint:

$$\dot{X} < \mathscr{V}_{\max}$$

$$\ddot{X} < \mathscr{A}_{\max} \tag{12}$$

Robot design constraint:

$$\theta_{\min} < \theta < \theta_{\max}$$

$$\dot{\theta}_{\min} < \theta < \dot{\theta}_{\max}$$

$$\ddot{\theta}_{\min} < \theta < \ddot{\theta}_{\max} \tag{13}$$

where $\mathscr{T}$ is the tolerance limit of the part, $\mathscr{V}_{\max}$ and $\mathscr{A}_{\max}$ are the velocity and acceleration limits of the extrusion head.

The proposed EEHQPP algorithm is shown in Table 1 where the part placement positions are assigned to the starting point of the part. In other words, the algorithm identifies the optimal starting point of the 3D printing path and thus the print geometry among the set of feasible starting points. To do so, first the path trajectories, printing parameters and robot specification are obtained. Next, a set of coordinates (each representing a starting print position) are generated in a discrete search space. A user-defined resolution is used while generating feasible positions. A higher resolution will yield a greater number of feasible points but as a trade-off can increase the computation time and the search space. Next, the search space is reduced by accounting for the collision and robot design constraints so that all the points along the path are within the robot's reach for a starting point/coordinate. The clearance is then added to prevent any potential collisions. In the next step, energy and error is calculated as described in Sections 2.1 and 2.2, respectively. The starting points which do not satisfy the quality constraints are removed and we obtain the feasible solutions. Among these feasible solutions, the point with the minimum energy is assigned as the optimal part location for printing.

3. Case study parameters

This section describes the adopted case study geometries and robot specifications for robotic additive manufacturing.

3.1. Experimental geometries

Two different geometries (illustrated in Fig. 3) are studied in this work:

Case 1. A square container of size (40 cm × 40 cm×10 cm) with a deviation tolerance limit of 1.5 mm.

Case 2. A spur gear with hub diameter of 22 cm, nominal diameter of 14 cm and overall length of 20 cm with a deviation tolerance limit of 1.1 mm.

Table 1
Energy-efficient high-quality part placement algorithm.

Step 1: Obtain the tool path, printing parameters and the type of robot.
Step 2: Generate feasible starting positions satisfying collision and robot design constraints.
Step 3: Calculate energy and quality to follow the defined tool path for all the starting points. Use print consistency constraint in calculations.
Step 4: Remove the starting points which do not satisfy the quality constraint.
Step 5: Find the starting point with minimum energy value.
Step 6: End.

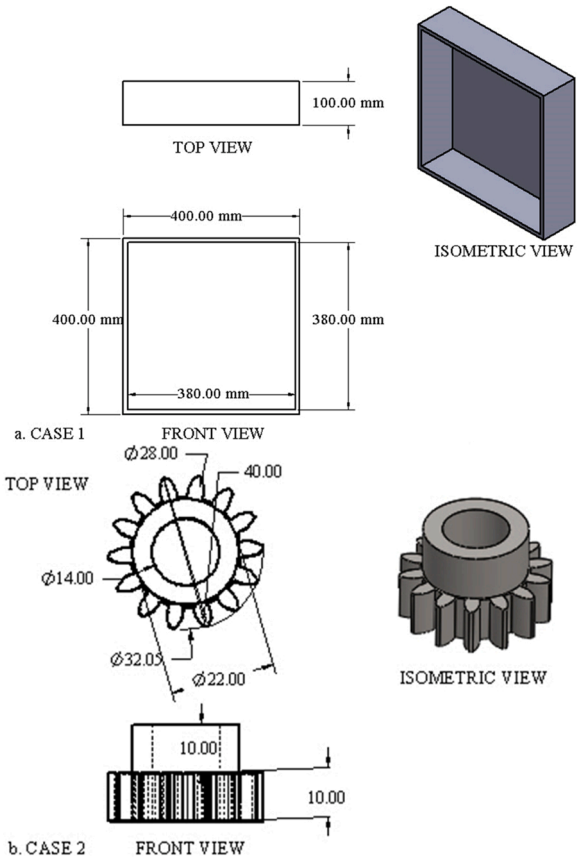

Fig. 3. The two different geometries in case study analysis: a. Case 1 (Container) and b. Case 2 (Gear).

3.2. Path planning

After the CAD model was created, slicing software Slic3r was used to generate the 3D printing path in the form of G-code instructions. The default print, printer, and filament settings of Slic3r were used for the Case 1. However, nozzle diameter was increased to 5 mm from 0.5 mm and layer height was increased to 1 mm from 0.3 mm to reduce the computation time in calculating energy values (by reducing the waypoint) for Case 2. Next, the G-code was used to extract the coordinates of the points for defining the trajectory for the extrusion head, which is attached to the end-effector of the robot manipulator. The number of extracted points along the trajectory for Cases 1 and 2 are 6,116 and 33,530, respectively.

3.3. Robot model and other model parameters

In this work, we consider 6 DOF ABB IRB 1600 model. The linear repeatability is 0.19 mm, and the linear accuracy is 1.03 mm. The specifications show that the printing linear accuracy is low in these

Table 2
Robot design constraints.

Robot	Range of movement	Length (in mm)	Mass (in kg)
Link 1	+ 180° to − 180°	486.5	101.19
Link 2	+ 120° to − 90°	150.0	26.40
Link 3	+ 65° to − 245°	700.0	41.45
Link 4	+ 200° to − 200°	300.0	7.3159
Link 5	+ 115° to − 115°	300.0	0.4599
Link 6	+ 400° to − 400°	80.0	0.03125

robots and hence, it is important to include accuracy or deviational error in the planning stage. The robot specifications are shown in Table 2.

The coordinate systems are divided into global and local coordinate system. The global coordinate system assumes that the robot base is at (382, 253, 0) and so the parts are placed accordingly. The local coordinate system is the system which assumes that the robot base is at (0, 0, 0). Fig. 4 shows the top view of the global coordinate system and the positioning of the robot base.

4. Results and discussion

The energy consumption and deviation error by six DOF robot is reported. All presented results are in local coordinates but are transferred to global coordinates before print execution. Java is used to formulate the energy and error values based on the proposed methodology in Section 2. To evaluate the performance of our proposed approach, we compare our solutions with a benchmark or base scenario which assumes that the part is located at the default coordinates determined by the commercial 3D printing software. A resolution of 0.01 m is used in this work. The optimal and default positions of part for two different cases with their energy and quality is shown in Table 3. For the container, the initial starting position had an energy value of 128.2 kJ, whereas the optimal starting position had an energy value of 119.9 kJ. This is a 6.5% reduction in energy consumption. Along with the improvement in energy consumption, the maximum deviation is also decreased. Similarly, for Case 2, energy consumption is decreased by 1.4%. Additionally, the quality of the part is significantly improved by placing the part in the optimal position rather than using the default position. In Cases 1 and 2, the maximum deviation error is reduced by 19.4% and 32.7%, respectively. This highlights the importance of considering both energy and quality metrics for optimal part placement.

Next, we compare the optimal solution by the EEHQPP output for each case, with respect to the coordinates of starting points that yield the extreme lowest energy and highest quality within the search space to further highlight the potential energy savings and quality enhancements that can be achieved. As expected, the lowest energy position is not necessarily the position with the highest quality as can be observed in Table 4 for Case 1 and Table 5 for Case 2. The number of feasible positions (search space) generated for placing the geometry in Cases 1 and 2 were 186 and 167 points, respectively. An energy map for all the feasible positions is created to better understand the energy consumed at different starting points for printing the Case 1 geometry, as shown in Fig. 5.

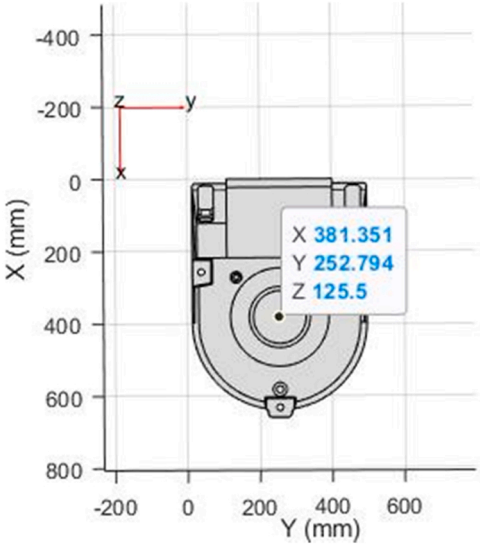

Fig. 4. Top view of the global coordinate system (point highlights the coordinates of topmost point on the robot base).

Table 3
Results of the proposed EEHQPP algorithm.

Description	Position	Case 1	Case 2
Location	Optimal	(−21, −20, 10)	(−11, 48.5, 10)
	Default	(−10.5, −10.4, 0.0)	(8.4, 8.4, 0)
Energy	Optimal	119.9 kJ	475.1 kJ
	Default	128.2 kJ	481.8 kJ
Maximum deviation error	Optimal	1.49 mm	1.049 mm
	Default	1.85 mm	1.56 mm

Table 4
Comparison between extreme and optimal placement positions for Case 1.

Starting position (x, y, z)	Description	Energy (kJ)	Maximum deviation error (mm)
(−21, −20, 10)	EEHQPP	119.9	1.49
(−10, −20, 20)	Lowest energy	76.9	2.16
(−71, 30, 10)	Highest quality	200.6	1.24

Table 5
Comparison between extreme and optimal placement positions for Case 2.

Starting position (x, y, z)	Description	Energy (kJ)	Maximum deviation error (mm)
(−11, 48.5, 10)	EEHQPP	475.1	1.049
(18.4, −11.5, 50)	Lowest energy	270.8	1.87
(8.5, 8.4, 0)	Highest quality	817.9	1.047

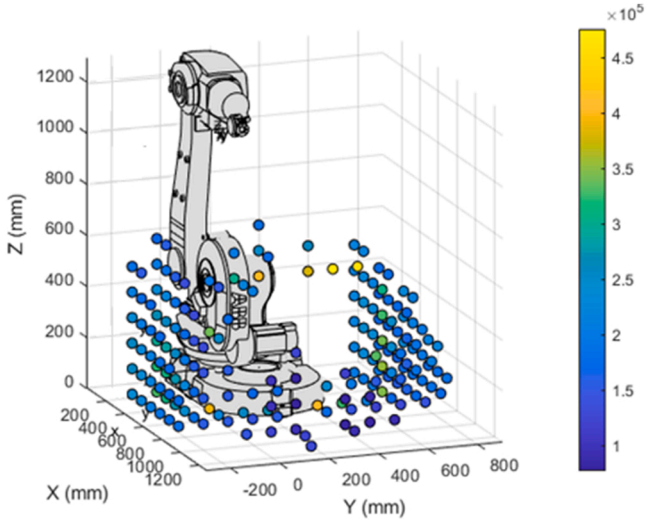

Fig. 5. Energy map for printing container.

In Case 2, the results are consistent with Case 1. The lowest quality placement has a high energy consumption whereas the lowest energy consumption position has large error, meaning that the printed part would be of bad quality. Among the 167 feasible points in the search space, 5 were within the tolerance limit of 1.1 mm. Fig. 6 shows the quality map of Case 2 based on a tolerance limit of 1.5 mm with 35 points highlighted as suitable starting points that can lead to good quality prints. Also, it can be seen from the Fig. 6, that as we move away from the robot's base, the quality is getting worse. That means, the quality is a function of distance between robot's base and part's printing location.

The computation time for calculating the energy and quality values

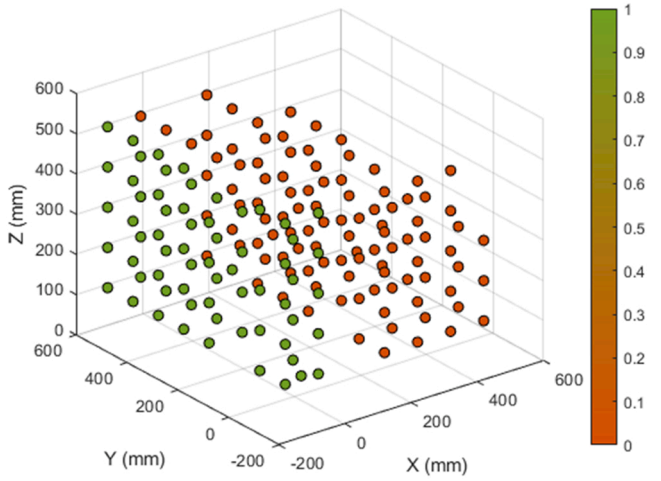

Fig. 6. Quality map for printing gear (Green: high quality and red: low quality).

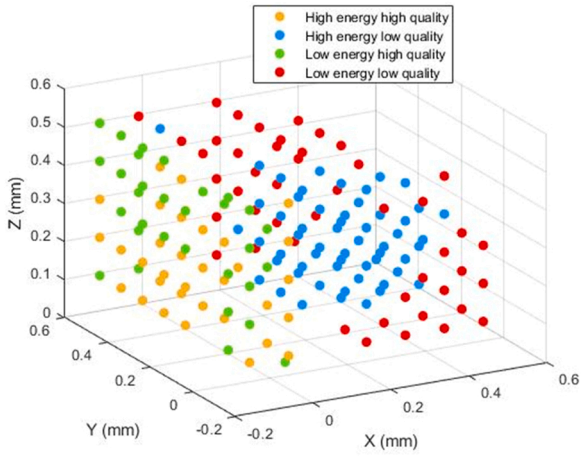

Fig. 7. The energy-quality map for Case 2 geometry.

for the Cases 1 and 2 geometries are 2 min and 13 min respectively. As the number of points along the trajectory are increased, we expect that the calculation time would increase. However, to reduce the calculation time, the number of time intervals between these points can be decreased. The EQ map is plotted for Case 2 in Fig. 7, where the normalized energy is calculated and cut off for low and high energy is 0.1. The EQ map will assist the operator in decision-making and finding the desired zones to place the parts based on both energy and quality criteria. It can also assist in deciding the orientation for bigger sized parts.

5. Conclusion

Robotic additive manufacturing is an emerging topic with various challenges and potentials towards next-generation collaborative robotic 3D printers for construction, defense, and space exploration applications. Before considering the dynamics/challenges introduced by multi-robot additive manufacturing systems, understanding the fundamentals of single-robot additive manufacturing and their challenges are necessary. In this work, an energy-efficient and quality-aware part positioning or placement for a single robot based on additive manufacturing is proposed. Energy and quality metrics are formulated (in form of 3D maps), and a systematic methodology based on single-objective optimization and energy-quality map is introduced to identify the optimal part placement within the robot's reach. Two cases for manufacturing a square container and a spur gear are studied. In both studies, the proposed methodology led to optimal part positions with significant reduction in energy and deviation error compared to the base/default scenario. More specifically, in Cases 1 and 2, the energy was reduced by 6.5% and 1.4% and the maximum deviation error is reduced by 19.4% and 32.7%, respectively. The established energy, quality, and energy-quality maps can guide users in identifying the optimum energy-efficient print locations based on the available tolerance limits. The proposed approach can also be used to other robot assisted manufacturing which have no external forces/torques acting on the robot.

With the increasing levels of capability and flexibility of industrial robots, ground [40] as well as aerial [41] mobility for manufacturing has seen growing interest among researchers. In the future, we will study the additive manufacturing of large-scale parts using a team of robots, in which the positioning and relocation of each robot will be studied concurrently. We expect that the inverse versions of the above maps would be critical in determining the optimal collaborative framework. Finally, as in this study deviation error is considered as a measure of quality, the incorporation of other quality metrics such as inter-layer and intra-layer bonding can be considered for future studies.

Declaration of Competing Interest

The authors declare that they have no known competing financial interests or personal relationships that could have appeared to influence the work reported in this paper.

References

[1] Urhal P, Weightman A, Diver C, Bartolo P. Robot assisted additive manufacturing: a review. Robot Comput Integr Manuf 2019;59:335–45. https://doi.org/10.1016/j.rcim.2019.05.005.
[2] Khosravani MR, Haghighi A. Large-scale automated additive construction: overview, robotic solutions, sustainability, and future prospect. Sustain 2022:14. https://doi.org/10.3390/su14159782.
[3] Li L, Haghighi A, Yang Y. A novel 6-axis hybrid additive-subtractive manufacturing process: Design and case studies. J Manuf Process 2018;33:150–60. https://doi.org/10.1016/j.jmapro.2018.05.008.
[4] Bin Ishak I, Fisher J, Larochelle P. Robot arm platform for additive manufacturing using multi-plane toolpaths. Proc ASME Des Eng Tech Conf 2016;5A-2016:1–7. https://doi.org/10.1115/DETC2016-59438.
[5] Bhatt PM, Kabir AM, Malhan RK, Shah B, Shembekar AV, Yoon YJ, et al. A robotic cell for multi-resolution additive manufacturing. Proc - IEEE Int Conf Robot Autom, 2019-May; 2019. p. 2800–7. https://doi.org/10.1109/ICRA.2019.8793730.
[6] Wu C, Dai C, Fang G, Liu YJ, Wang CCL. RoboFDM: a robotic system for support-free fabrication using FDM. Proc - IEEE Int Conf Robot Autom 2017:1175–80. https://doi.org/10.1109/ICRA.2017.7989140.
[7] Calabrese M, Primo T, Del Prete A, Filitti G. Nesting algorithm for optimization part placement in additive manufacturing. Int J Adv Manuf Technol 2022;119:4613–34. https://doi.org/10.1007/s00170-021-08130-y.
[8] Ye C, Yang J, Zhao H, Ding H. Task-dependent workpiece placement optimization for minimizing contour errors induced by the low posture-dependent stiffness of robotic milling. Int J Mech Sci 2021;205:106601. https://doi.org/10.1016/j.ijmecsci.2021.106601.
[9] Fry NR, Richardson RC, Boyle JH. Robotic additive manufacturing system for dynamic build orientations. Rapid Prototyp J 2020;26:659–67. https://doi.org/10.1108/RPJ-09-2019-0243.
[10] Ji W, Wang L. Industrial robotic machining: a review. Int J Adv Manuf Technol 2019;103:1239–55. https://doi.org/10.1007/s00170-019-03403-z.
[11] Iglesias I, Sebastián MA, Ares JE. Overview of the state of robotic machining: current situation and future potential. Procedia Eng 2015;132:911–7. https://doi.org/10.1016/j.proeng.2015.12.577.
[12] Bhatt PM, Kulkarni A, Malhan RK, Gupta SK. Optimizing part placement for improving accuracy of robot-based additive manufacturing. Proc - IEEE Int Conf Robot Autom 2021:859–65. https://doi.org/10.1109/ICRA48506.2021.9561494.
[13] Chen C, Peng F, Yan R, Li Y, Wei D, Fan Z, et al. Stiffness performance index based posture and feed orientation optimization in robotic milling process. Robot Comput Integr Manuf 2019;55:29–40. https://doi.org/10.1016/j.rcim.2018.07.003.
[14] Caro S, Dumas C, Garnier S, Furet B. Workpiece placement optimization for machining operations with a KUKA KR270-2 robot. Proc - IEEE Int Conf Robot Autom 2013:2921–6. https://doi.org/10.1109/ICRA.2013.6630982.
[15] Wu K, Li J, Zhao H, Zhong Y. Review of industrial Robot Stiffness identification and modelling. Appl Sci 2022:12. https://doi.org/10.3390/app12178719.
[16] FarzanehKaloorazi MH, Bonev IA, Birglen L. Simultaneous path placement and trajectory planning optimization for a redundant coordinated robotic workcell. Mech Mach Theory 2018;130:346–62. https://doi.org/10.1016/j.mechmachtheory.2018.08.022.

[17] Pardi T, Ortenzi V, Fairbairn C, Pipe T, Esfahani AMG, Stolkin R. Planning maximum-manipulability cutting paths. IEEE Robot Autom Lett 2020;5:1999–2006. https://doi.org/10.1109/LRA.2020.2970949.
[18] Bhatt PM, Nycz A, Gupta SK. Optimizing Multi-Robot Placements for Wire Arc Additive Manufacturing. 2022 Int. Conf. Robot. Autom. IEEE; 2022. p. 7942–8. https://doi.org/10.1109/ICRA46639.2022.9812318.
[19] Guerra-Zubiaga DA, Luong KY. Energy consumption parameter analysis of industrial robots using design of experiment methodology. Int J Sustain Eng 2021;14:996–1005. https://doi.org/10.1080/19397038.2020.1805040.
[20] Kraljić D, Kamnik R. Trajectory planning for additive manufacturing with a 6-DOF industrial robot. Mech Mach Sci 2019;67:456–65. https://doi.org/10.1007/978-3-030-00232-9_48.
[21] Zanchettin AM, Lacevic B. Safe and minimum-time path-following problem for collaborative industrial robots. J Manuf Syst 2022;65:686–93. https://doi.org/10.1016/j.jmsy.2022.10.020.
[22] Bi ZM, Wang L. Optimization of machining processes from the perspective of energy consumption: a case study. J Manuf Syst 2012;31:420–8. https://doi.org/10.1016/j.jmsy.2012.07.002.
[23] Wang X, Yan Y, Gu X. Spot welding robot path planning using intelligent algorithm. J Manuf Process 2019;42:1–10. https://doi.org/10.1016/j.jmapro.2019.04.014.
[24] Carabin G, Wehrle E, Vidoni R. A review on energy-saving optimization methods for robotic and automatic systems. Robotics 2017:6. https://doi.org/10.3390/robotics6040039.
[25] Nonoyama K, Liu Z, Fujiwara T, Alam MM, Nishi T. Energy-efficient robot configuration and motion planning using genetic algorithm and particle swarm optimization. Energies 2022:15. https://doi.org/10.3390/en15062074.
[26] Gürel S, Gultekin H, Emiroglu N. Scheduling a dual gripper material handling robot with energy considerations. J Manuf Syst 2023;67:265–80. https://doi.org/10.1016/j.jmsy.2023.01.011.
[27] Bukata L, Šůcha P, Hanzálek Z. Optimizing energy consumption of robotic cells by a Branch & Bound algorithm. Comput Oper Res 2019;102:52–66. https://doi.org/10.1016/j.cor.2018.09.012.
[28] Haghighi A, Mohammed A, Wang L. Energy efficient multi-robotic 3D printing for large-scale construction – framework, challenges, and a systematic approach 2021; vol. Volume 2. https://doi.org/10.1115/MSEC2021-63787.
[29] Ma Z, Gao M, Wang Q, Wang N, Li L, Liu C, et al. Energy consumption distribution and optimization of additive manufacturing. Int J Adv Manuf Technol 2021;116:3377–90. https://doi.org/10.1007/s00170-021-07653-8.
[30] Jiang J, Xu X, Stringer J. Optimization of process planning for reducing material waste in extrusion based additive manufacturing. Robot Comput Integr Manuf 2019;59:317–25. https://doi.org/10.1016/j.rcim.2019.05.007.
[31] Mohammed A, Schmidt B, Wang L, Gao L. Minimizing energy consumption for robot arm movement. Procedia CIRP 2014;25:400–5. https://doi.org/10.1016/j.procir.2014.10.055.
[32] Paryanto Brossog M, Bornschlegl M, Franke J. Reducing the energy consumption of industrial robots in manufacturing systems. Int J Adv Manuf Technol 2015;78:1315–28. https://doi.org/10.1007/s00170-014-6737-z.
[33] Gadaleta M, Pellicciari M, Berselli G. Optimization of the energy consumption of industrial robots for automatic code generation. Robot Comput Integr Manuf 2019;57:452–64. https://doi.org/10.1016/j.rcim.2018.12.020.
[34] Liu A, Liu H, Yao B, Xu W, Yang M. Energy consumption modeling of industrial robot based on simulated power data and parameter identification. Adv Mech Eng 2018;10. https://doi.org/10.1177/1687814018773852.
[35] Mohammed A, Schmidt B, Wang L. Energy-efficient robot configuration for assembly. J Manuf Sci Eng 2017;139:1–7. https://doi.org/10.1115/1.4034935.
[36] Spong MW, Hutchinson S, Vidyasagar M. Robot modeling and control, vol. 3. New York: Wiley; 2006.
[37] K L Conrad, T C Yih, 2000. Robotic Calibration Issues: Accuracy, Repeatability and Calibration. 8th Mediterr. Conf. Control Autom., Patras, Greece: IEEE; 2000, p. 1719.
[38] Yang Y, Liu X, Kan C. Point cloud based online detection of geometric defects for the certification of additively manufactured mechanical metamaterials. J Manuf Syst 2022;65:591–604. https://doi.org/10.1016/j.jmsy.2022.09.011.
[39] Giberti H, Sbaglia L, Urgo M. A path planning algorithm for industrial processes under velocity constraints with an application to additive manufacturing. J Manuf Syst 2017;43:160–7. https://doi.org/10.1016/j.jmsy.2017.03.003.
[40] Dörfler K, Dielemans G, Lachmayer L, Recker T, Raatz A, Lowke D, et al. Additive manufacturing using mobile robots: opportunities and challenges for building construction. Cem Concr Res 2022:158. https://doi.org/10.1016/j.cemconres.2022.106772.
[41] Perez-Grau FJ, Martinez-de Dios JR, Paneque JL, Acevedo JJ, Torres-González A, Viguria A, et al. Introducing autonomous aerial robots in industrial manufacturing. J Manuf Syst 2021;60:312–24. https://doi.org/10.1016/j.jmsy.2021.06.008.